Olfactory coding in the antennal lobe of the bumble bee Bombus terrestris

Marcel Mertes, Julie Carcaud, Jean-Christophe Sandoz

scientific reports

Check for updates

OPEN

Olfactory coding in the antennal lobe of the bumble bee *Bombus terrestris*

Marcel Mertes[1,3], Julie Carcaud[2,3]✉ & Jean-Christophe Sandoz[2]

Sociality is classified as one of the major transitions in evolution, with the largest number of eusocial species found in the insect order Hymenoptera, including the Apini (honey bees) and the Bombini (bumble bees). Bumble bees and honey bees not only differ in their social organization and foraging strategies, but comparative analyses of their genomes demonstrated that bumble bees have a slightly less diverse family of olfactory receptors than honey bees, suggesting that their olfactory abilities have adapted to different social and/or ecological conditions. However, unfortunately, no precise comparison of olfactory coding has been performed so far between honey bees and bumble bees, and little is known about the rules underlying olfactory coding in the bumble bee brain. In this study, we used in vivo calcium imaging to study olfactory coding of a panel of floral odorants in the antennal lobe of the bumble bee *Bombus terrestris*. Our results show that odorants induce reproducible neuronal activity in the bumble bee antennal lobe. Each odorant evokes a different glomerular activity pattern revealing this molecule's chemical structure, i.e. its carbon chain length and functional group. In addition, pairwise similarity among odor representations are conserved in bumble bees and honey bees. This study thus suggests that bumble bees, like honey bees, are equipped to respond to odorants according to their chemical features.

Sociality is classified as one of the major transitions in evolution, and animals often form social groups because the benefits (either direct or indirect) of grouping outweigh the costs of breeding independently. In bees, eusociality is notably found in the corbiculate bees (bees with concave "pollen baskets" on their hind legs) which include well-known eusocial taxa, the Apini (honey bees) and the Bombini (bumble bees). The 'primitively eusocial' bumble bees (*Bombus* spp.) share some traits with advanced eusocial species, like honey bees, but lack particular aspects that would qualify them as advanced eusocial organisms[1].

Bumble bees and honey bees, although both polylectic foragers, differ in many ways and show notable ecological differences[1]. Bumble bee colonies are annual and small (from dozens to a hundred individuals) compared to the perennial honey bee colonies which contain many thousands of individuals. Division of labor in the colony also differs between honey bees and bumble bees. In honey bees, workers progress through various nest- and foraging tasks in an age-dependent fashion whereas in bumble bees, workers of all ages and sizes may perform nest or foraging duties[2]. Social communication also differs, while both species use a number of pheromones within the nest, honey bees developed a unique symbolic communication system (the well-known dance language) to inform each other about the location of food sources[3]. In the same context, bumble bees gather information from "excited runs" and pheromone signals provided by foragers returning to the nest[4–6].

Chemosensation plays a major role in social interactions in insect societies, and is also critical for bees' foraging success. Given the differences in social organization and foraging strategies existing between bumble bees and honey bees, we might expect important differences in how the two species process olfactory information. In insects, odorants are detected by olfactory receptors (ORs) carried by olfactory sensory neurons (OSNs) on the antennae (Fig. 1A). ORs belong to a multigenic family whose members are known to evolve quickly through complex patterns of gene birth and death[7]. Comparative analyses of the genomes of a honey bee (*A. mellifera*) and two bumble bee species (*B. impatiens* and *B. terrestris*) demonstrated that bumble bees have a slightly lower number of ORs than honey bees. Conversely, however, bumble bees possess an expanded repertoire of gustatory receptors (GRs) compared to honey bees[1], suggesting different priorities in the chemosensory systems of the two insects. Apart from absolute numbers, substantial differences are found between honey bees' and bumble

[1]Department of Neurobiology and Center of Excellence "Cognitive Interaction Technology", Bielefeld University, 33615 Bielefeld, Germany. [2]Evolution, Genomes, Behavior and Ecology, CNRS, IRD, Université Paris-Saclay, Gif-sur-Yvette, France. [3]These authors contributed equally: Marcel Mertes and Julie Carcaud. ✉email: julie.carcaud@egce.cnrs-gif.fr

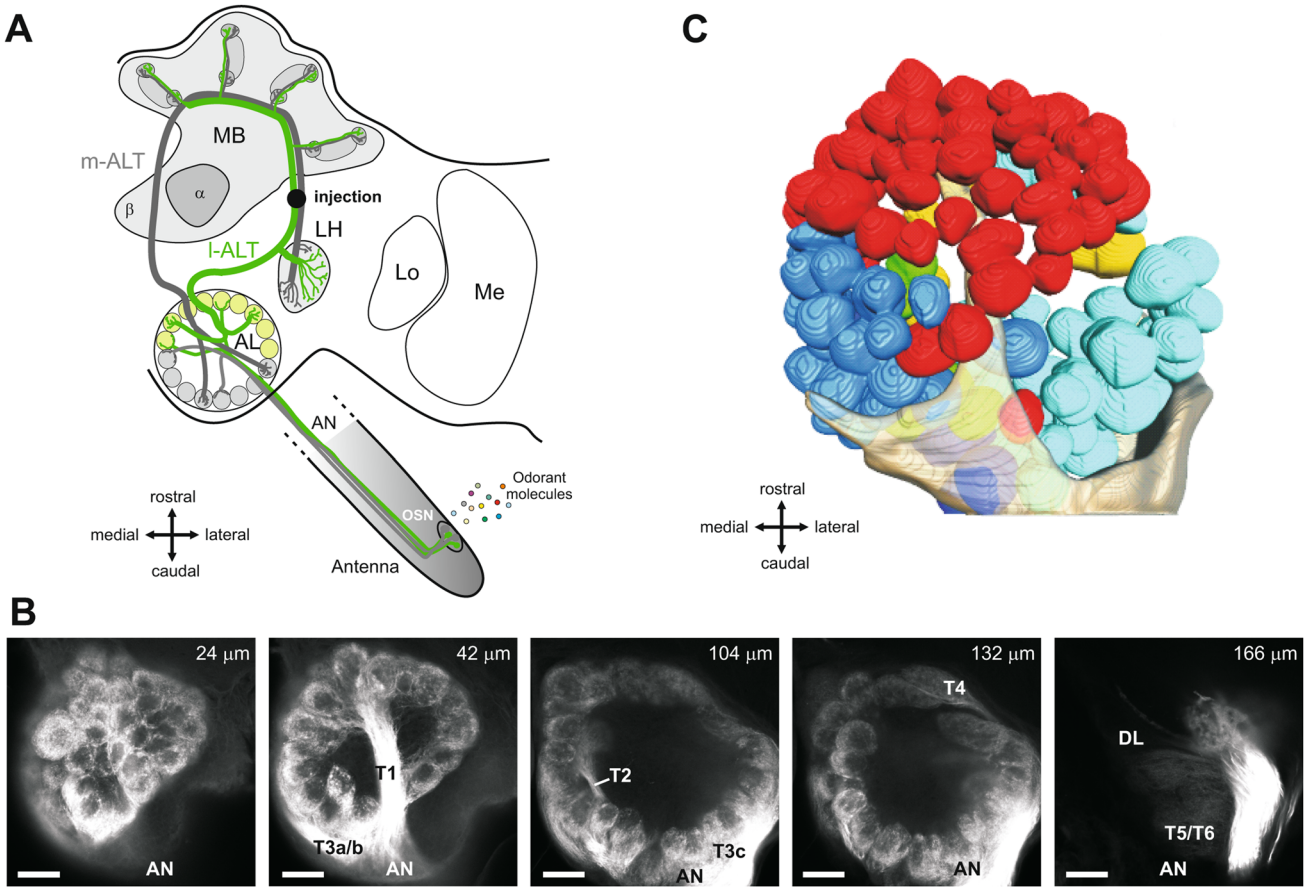

Figure 1. Anatomy of the bumble bee antennal lobe (AL). (**A**) Hymenopteran dual olfactory pathway (adapted from Carcaud et al. 2012). Odorant molecules are detected by olfactory sensory neurons (OSNs) on the antenna, which form the antennal nerve (AN) and send olfactory information to the primary olfactory center, the antennal lobe (AL). Then, projection neurons (PNs) convey information to higher-order centers, the mushroom bodies (MB) and the lateral horn (LH), using two main tracts, the l-ALT (lateral antennal-lobe tract, in green) and the m-ALT (medial antennal-lobe tract, in grey). PNs of the m-ALT and l-ALT project to distinct areas in the MB and in the LH. The black dot indicates the site of injection for calcium imaging. Lo: lobula, Me: medulla, α: α-lobe, β: β-lobe. (**B**) Confocal image sequence through a bumble bee antennal lobe (left lobe) obtained by anterograde antennal staining (using tetramethylrhodamine dextran). The scale bars indicate a length of 50 µm. The depth along the z-axis of the confocal images are indicated on the top right of each image. AN: antennal nerve. T1-T4: subdivisions of the antennal nerve in the AL. (**C**) Three-dimensional reconstruction of the 158 glomeruli in the antennal lobe presented in B. The glomeruli are colored depending on their input tracts. The numbers of glomeruli per input tracts are: T1 = 60 (red), T2 = 7 (green), T3a = 27 (medium blue), T3b = 16 (dark blue), T3c = 42 (turquoise), and T4 = 7 (yellow) glomeruli. The antennal nerve is shown in semi-transparent coloring.

bees' OR repertoires, with a limited number of ortholog genes. These observations suggest that their olfactory abilities have adapted to different social and/or ecological conditions. Unfortunately, no precise comparison of olfactory coding has been performed so far between honey bees and bumble bees.

Olfactory coding and processing have been intensively studied in the honey bee, a traditional animal model in neuroethology[8–11]. In addition to extensive research on honey bees' olfactory behaviors[12–14], this insect's olfactory pathways have been described in great details[15–17] and physiological recordings like electrophysiology[18,19] and optical imaging[20–24] have unraveled the rules of odor coding. By contrast, less work has been devoted to the understanding of olfactory perception and learning in bumble bees, and most of this work used behavioral approaches[25–28]. A number of studies have started to describe the anatomy of the bumble bee brain[29–33]. Its general architecture has been found to be highly similar to that of the honey bee, in particular with regards to the olfactory pathway[32,33]. In both species, OSN project from the antenna to the primary olfactory center, the antennal lobe (AL), constituted of spherical anatomical and functional units, the glomeruli (~ 165 in honey bees)[34]. Within the AL, local interneurons perform local computations[35], and projection neurons (PNs) then convey processed information to higher-order centers, the mushroom bodies and the lateral horn. In honey bees and bumble bees, as in most Hymenoptera, the PNs are divided in two main tracts of uniglomerular neurons, the lateral antennallobe tract (l-ALT) and the medial antennal lobe tract (m-ALT)[15,32,36], with possibly different functions[18,37,38]. Apart from the observation of a general similarity in the architecture of the olfactory pathway,

functional studies of odor coding in bumble bees are scarce. In the 1980's, two studies described bumble bees' peripheral equipment in cuticular sensilla on the antennae and performed electroantennogram (EAG) recordings of their antenna, showing that it responds to a wide range of volatiles, including both floral and pheromonal odorants[39,40]. These approaches were used again later to show that sensillar equipment and olfactory sensitivity increase with worker size in bumble bees[41] as well as to study left–right asymetries[42]. With regards to neural odor coding, one study demonstrated the existence of glomerulus-size odor-induced oscillations in the bumble bee AL[43]. More recently, extracellular recordings of AL neurons showed reproducible responses to odorants, and observed a specific response pattern for a pheromonal compound compared to other odorants[32]. Apart from these findings, little is known about the rules underlying olfactory coding in the bumble bee brain.

In the present work, we used in vivo calcium imaging to study olfactory coding by l-ALT PNs in the AL of the bumble bee *Bombus terrestris.* To compare odor-coding rules in bumble bees and honey bees, we presented a panel of floral odorants previously used in studies on olfactory processing and perception in honey bees[13,38,44]. Our results show that odorants induce reproducible neuronal activity in the bumble bee antennal lobe. Each odorant evokes a different glomerular activity pattern depending on the molecules' chemical structure, i.e. carbon chain length and functional group. Odor-similarity relationships in the bumble bee AL are highly correlated to those found in the honey bee AL.

Results

Anatomy of the bumble bee antennal lobe. *Olfactory sensory neuron innervation.* Using fluorescent tracers, we performed mass staining of olfactory sensory neurons (OSNs) in the bumble bee *Bombus terrestris* (Fig. 1A). The tracers migrated along the antennal nerve until the OSNs' axonal projections in the cortex (outer layer) of the glomeruli in the AL. As previously reported[33], we found a similar arrangement of sensory tracts in the bumble bee antennal lobe as in the honey bee. The most prominent tract, T1, is easily identifiable, crossing the center of the antennal lobe from the antennal nerve caudally (Fig. 1B) to the most ventral and rostral part of the antennal lobe where it innervates many glomeruli. The T3 tract is also prominent, leaving the antennal nerve on the caudal side of the antennal lobe, propagating medially on its outskirts and innervating many glomeruli on the dorso-caudal region. T3 divides itself into at least 3 sub-branches: two running medially (T3a and T3b) and innervating many medial glomeruli, and one running laterally (T3c) innervating caudo-lateral glomeruli. Tract T2 is a much smaller tract that goes from the nerve entrance through the medial part of the lobe neuropil at approximately half depth and innervates only a few medial glomeruli. Tract T4 is another smaller tract, which runs laterally along the outer side of the glomerular region, and innervates a set of tear-shaped glomeruli on the most dorsal part of the antennal lobe, close to the dorsal lobe. Contrary to other glomeruli with a clearly stained cortex, these T4 glomeruli are characterized by a homogeneous staining of sensory neurons. A conspicuous tract of neurons bypasses the antennal lobe completely on its dorso-lateral side and forms the two tracts innervating the dorsal lobe (T5) and the subesophageal zone (T6) that transmit mechanosensory and gustatory information respectively. Single glomeruli from the confocal images were reconstructed (Fig. 1C) and we found 158 ± 4 glomeruli in the antennal lobe of bumble bees (n = 4 bumble bees), a slightly lower number compared to honey bees (~ 160–166 glomeruli)[15,45,46], which roughly corresponds to the number of OR genes found in bumble bees[1]. We observed that in bumble bees, as in honey bees, the outer surface of the antennal lobe consists of a single layer of glomeruli. This arrangement is particularly well adapted to optical measurements of glomerular activity (see below).

Projection neuron innervation. Further similarities between honey bee and bumble bee olfactory systems were observed at the level of projection neurons innervation[32]. Using the classical technique used in honey bees[38,47], we stained the lateral antennal-lobe tract (l-ALT) of projection neurons (Fig. 1A). By introducing tracers into the protocerebrum at a location lateral to the α-lobe of the mushroom bodies and rostral to the lateral horn, we obtained clear staining of l-ALT PNs (Fig. 2A) in rostro-ventral glomeruli of the antennal lobe (Fig. 1C, red glomeruli innervated by T1 mainly). In contrast to anterograde staining of OSNs, PN staining was found to be homogeneous in the whole volume of the glomeruli, with PN somata visible on the edge of the glomerular area of the AL (Fig. 2A).

All these observations confirm that OSN and l-ALT PN glomerular innervations are highly similar in bumble bees compared to the ones observed in the honey bee olfactory system. We then wondered whether similar olfactory coding rules are found in the two olfactory systems.

In vivo *calcium imaging*. We performed in vivo calcium imaging measurements in 14 bumble bee AL using the calcium indicator Fura-2 dextran, and recorded calcium responses from the dendrites of l-ALT PNs in rostro-ventral glomeruli (T1 region). We studied the coding of floral odorants. Inspired by previous work on honey bee olfactory perception and coding[13,38,44,47], we presented to the bumble bees a set of 16 odorants differing systematically in their functional group and chain length.

Intensity of odor-induced responses. All odorants induced remarkable activity in a combination of AL glomeruli, while air control stimulation had no effect (Figs. 2B, 3A; n = 14; RM-ANOVA, $F_{16, 208} = 17.1$, $p < 0.0001$, comparisons to the control: Dunnett test, $p < 0.01$). As the odorants systematically varied in terms of chemical group and carbon chain length, we evaluated the effect of these properties on the intensity of calcium responses. Odorants with different functional groups induced different activity levels (Fig. 3B, RM-ANOVA $F_{3,39} = 22.1$, $p < 0.0001$). Among functional groups, the weakest responses were evoked by primary alcohols, which induced significantly lower responses than the other chemical groups (Tukey HSD test: $p < 0.01$ compared to secondary alcohols and $p < 0.001$ compared to ketones and aldehydes), which did not differ from each other. Odorants

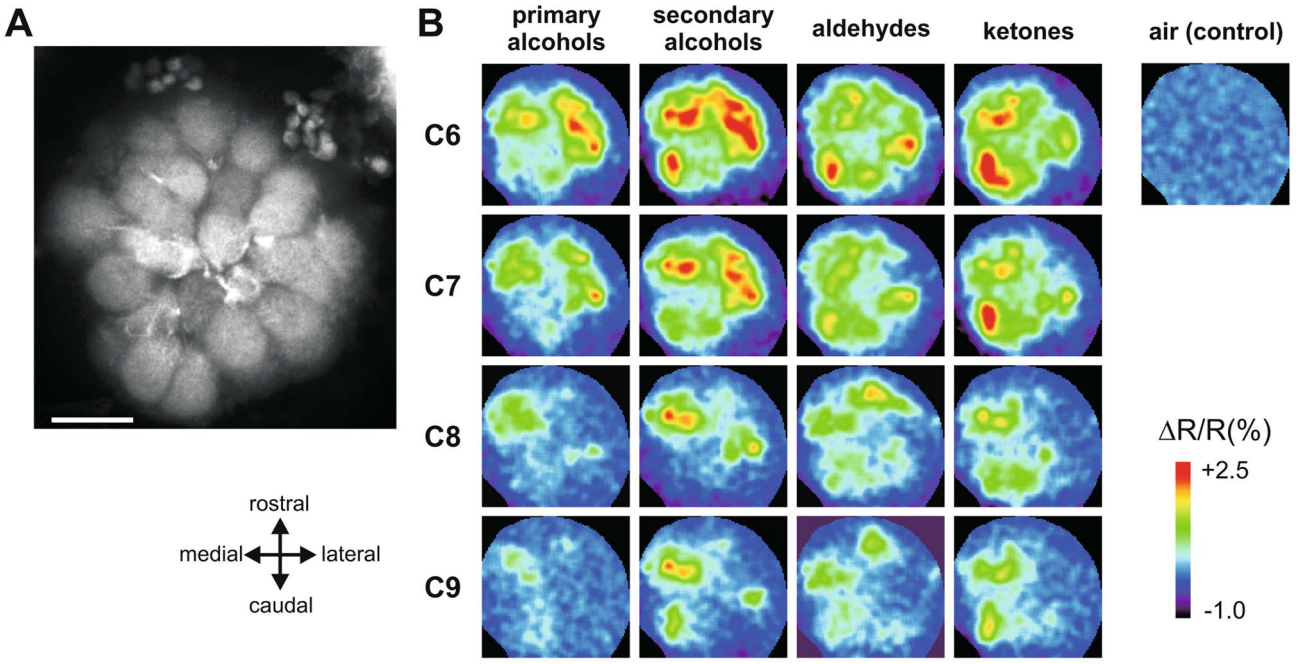

Figure 2. Odor-induced calcium signals from glomeruli innervated by the lateral antennal-lobe tract (l-ALT). (**A**) Confocal image (z-projection over 14 µm, from 6 to 20 µm depth) of the superior part of the AL after retrograde staining (using tetramethylrhodamine dextran) of l-ALT PNs. Fluorescence coming from dendrites of l-ALT PNs is clearly visible in all observed glomeruli. (**B**) Calcium signals in the AL evoked by a panel of 16 odorants varying systematically according to their carbon chain length (C6–C9) and their functional group (primary and secondary alcohols, aldehydes and ketones). Relative fluorescence changes (ΔR/R%) are presented in a false-color code, from dark blue (no response) to red (maximal response). Different odorants induce different glomerular activity patterns.

with different chain lengths also induced different activity levels (Fig. 3C, RM-ANOVA, $F_{3,39} = 14.4$, $p < 0.0001$). Generally, global response intensity decreased with increasing chain length, i.e. odorant molecules with 6 and 7 carbons induced stronger neural activity than odorants with 8 and 9 carbons (Tukey HSD test: a vs. b: $p < 0.01$). This pattern of results recapitulates the observations made in honey bees[38,44,47] and can be explained by the volatility of the odorants, as measured by their individual vapor pressure. Indeed, AL response was highly correlated to vapor pressure (Fig. 3D, $R^2 = 0.88$, $F_{1,14} = 106.7$, $p < 0.0001$) confirming that the more volatile the odorant (i.e. the larger its vapor pressure), the more molecules were present in headspace in the sample and the larger was the recorded AL response to this odorant. In the presented odorant panel, alcohols and molecules with longer carbon chains possess lower volatility and thus induced lower responses.

Similarity among odor response maps. We then evaluated how chemical characteristics of odorants affected similarity relationships among AL response maps. We thus calculated a measure of (dis-)similarity between response maps (pixelwise Euclidian distance) for all possible pairs of the 16 tested odorants, and produced a distance matrix, which provides an overview of similarity relationships among these odorants (Fig. 4). The more similar odor responses were between two odorants, the smaller are the Euclidian distances and the more intense is the color in the matrix. The matrix reveals a strong effect of the odorant's carbon chain length on similarity relationships, as shown by the red diagonal lines in the matrix (e.g. for primary alcohols vs. secondary alcohols). Generally, distances between any two odorants of the same carbon chain length were smaller than distances between odorants with different carbon chain lengths. A remarkable exception was observed with secondary alcohols which appeared to be closer to the primary alcohol with a shorter chain by one C atom (see[44,47] for a similar effect in honey bees). The matrix also suggests that odor pairs with longer carbon chains (C8 vs. C9) evoke more similar activation patterns (i.e. smaller Euclidian distances) than odor pairs with shorter carbon chain length (C6 vs. C7). This more pronounced similarity is also visible in single recordings, as for example shown in Fig. 2B, where a distinct change in the glomerular activity map can be seen between C7 and C8 odorants, but not between C6 and C7 or between C8 and C9 molecules. Odorants' functional group also plays a role in similarity relationships, although this effect is less easily visible in the matrix. Some pairs of functional groups show higher similarity than others, for instance most primary and secondary alcohols show a high similarity (low distance).

We confirmed these observations by performing multidimensional analyses using these Euclidian distance measures (Fig. 5). A hierarchical cluster analysis using Ward's classification method (Fig. 5A) showed that the odorants formed three main clusters. Odorants primarily segregated along two branches. The upper branch predominantly grouped odorants with short carbon chain lengths (C6 and C7). Within this branch, odorants were

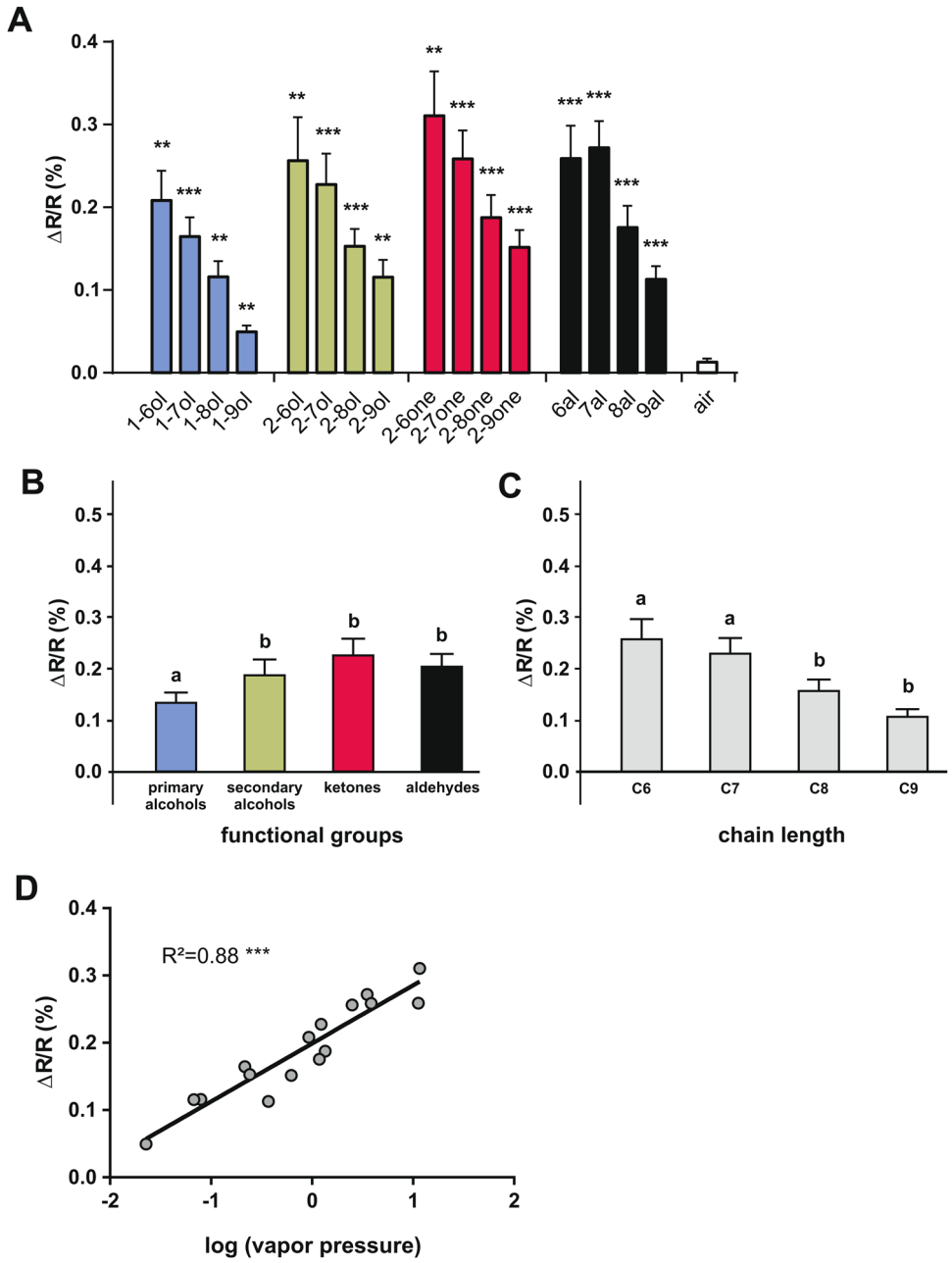

Figure 3. Intensity of calcium responses to 16 aliphatic odorants. (**A**) Amplitude of calcium responses (ΔR/R%) recorded in l-APT PNs to the 16 different odorants. All odors induce significant activity in comparison to the air control (n = 14, $p < 0.01$). (**B**) Mean amplitude of calcium responses (ΔR/R%) to different odorants according to their functional group (primary and secondary alcohols, aldehydes, and ketones). Primary alcohols (in blue) induced weaker activity than the other functional groups (n = 14, $p < 0.01$). (**C**) Amplitude of calcium responses (ΔR/R%) depending on odorants' carbon chain length (6, 7, 8, and 9 carbons). Odorants with the longest carbon chain (C8 and C9) induced weaker activation than odorants with a short carbon chain (C6 and C7) (n = 14, $p < 0.01$). (**D**) Amplitude of calcium responses (ΔR/R%) induced by each of the 16 aliphatic odorants as a function of its vapor pressure (in log units). The linear regression shows a significant correlation ($R^2 = 0.88$, $p < 0.001$).

grouped according to their functional groups, with primary and secondary alcohols in one subgroup (C–OH functional group) and aldehydes and ketones in the other (C=O functional group). The lower branch exclusively contained odorants with longer carbon chain lengths (C8 and C9). Within this branch, odorants also tended to be distributed according to their functional group, apart from 1-nonanol. This analysis shows, as can be seen in the matrix (Fig. 4) as well as in individual recordings (Fig. 2B), that long-chain molecules evoke highly similar activity patterns, which are less dependent on the functional group than shorter molecules.

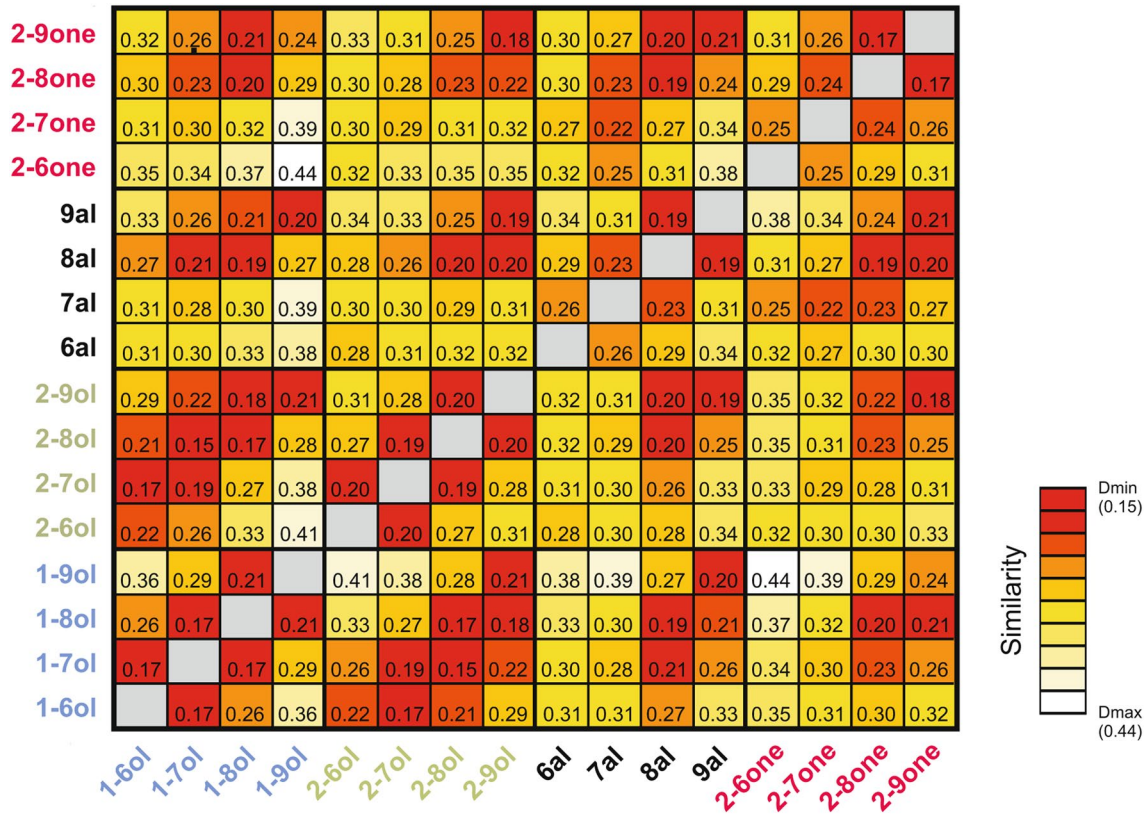

Figure 4. Similarity relationships among the 16 odorants. The matrix shows in a false-color code the Euclidian distances for the 120 odorant pairs. Higher similarity (shorter distances, D_{min}) is represented in red, while lower similarity (longer distances, D_{max}) is shown in lighter colors (white and yellow). The matrix shows generally higher similarity (smaller distances) among odorants with a long carbon chain length (C8 and C9, e.g. 8al vs. 2-9one or 9al vs. 1-8ol) compared to the corresponding odor pair combinations within shorter chain lengths, i.e. C6 and C7. High similarity is also observed between primary and secondary alcohols, along a diagonal line showing a dependency on chain length (lower left side of the matrix).

We next performed a multidimensional scaling analysis[48], using the Euclidian distance matrix, to understand the most meaningful dimensions underlying similarity relationships among odorants, focusing on the 3 main dimensions (Fig. 5B). Dimension 1 mostly provided information about odorants' carbon chain length, as odorants are represented along this axis by increasing carbon chain length for all functional groups (Fig. 5B left). Dimension 2 contained both functional group and chain length information. Primary and secondary alcohols were not separated from each other, but these C–OH functional groups were clearly separated from both ketones and aldehydes with a C=O functional group (Fig. 5B left). Dimension 2 also contains carbon chain length information for primary and secondary alcohols, as the odorants are represented along this axis by increasing carbon chain length. Lastly, dimension 3 clearly separates aldehydes (lower values) from ketones, primary and secondary alcohols (higher values, Fig. 5B right). To summarize, the three main dimensions of the multidimensional scaling analysis represented odorants' chain length and functional group information, distinguishing alcohols, ketones and aldehydes from each other.

The observations made on the distance matrix (Fig. 4) and the multidimensional analysis (Fig. 5) are supported by statistical analyses (Fig. 6). First, odor-specific coding is demonstrated by the fact that odor response maps for presentations of the same odorant were more similar (smaller Euclidian distances) than odor response maps for presentations of two different odorants (Fig. 6A, Paired t-test, $t = 6.94$, $p < 0.0001$, 13 df). Second, odorants with the same functional group induced significantly more similar odor response maps compared to odorants with different functional groups (Fig. 6B, Paired t-test, $t = 4.69$, $p < 0.001$). Lastly, odorants with the same carbon chain length induced more similar response maps than odorants with different carbon chain lengths (Fig. 6C, Paired t-test, $t = 4.99$, $p < 0.001$). This effect increased with the difference in the number of carbon atoms between the odorant molecules (Fig. 6D). The difference between odor maps was thus stronger when the molecules differed by at least 2 carbons, i.e. C6 vs. C8 or C6 vs. C9 (ANOVA $F_{3,39} = 25.86$, $p < 0.0001$; Tukey HSD test: a vs. b $p < 0.01$; a vs. c $p < 0.001$). These analyses thus demonstrate that odor coding in the bumble bee AL relies on both odorants' chain length and odorant's functional group.

Euclidian distances measure (dis-)similarity between odor-response maps by taking into account differences both in the pattern of activated regions (glomeruli) and in intensity between responses. To concentrate more on the activity patterns, these analyses were also performed by using the correlation coefficient between pixel responses as a measure of similarity between odor-response maps. These analyses provided exactly the same results. First, correlation coefficients were higher (i.e. the maps were more similar) for presentations of the same

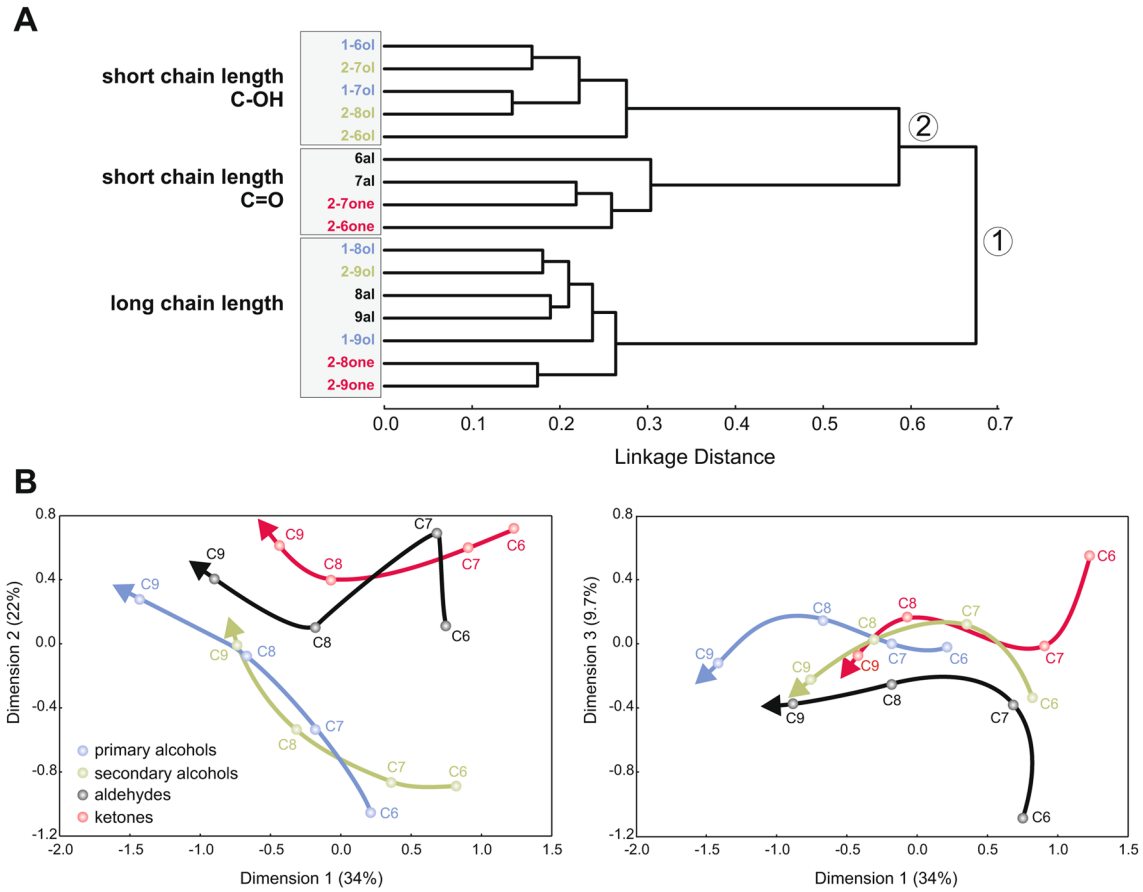

Figure 5. Multidimensional analyses. (**A**) Cluster analysis showing similarity relationships among odorant response maps (Ward's classification method). Short linkage distance between branches indicates odorants with similar response maps. Functional groups are shown in different colors: primary alcohols in blue, secondary alcohols in green, aldehydes in black, and ketones in red. The analysis shows a first separation (node 1) between odorants with short and long carbon chain lengths. Odorants with a short carbon chain are then subdivided (node 2) into alcohols (primary and secondary, C–OH functional group) and ketones/aldehydes (C = O functional group). (**B**) Multidimensional scaling analysis based on the Euclidian distance matrix for the 16 odorants. The first dimension (left panel) explains 34% of overall variance and orders molecules according to their chain length from short (on the right, C6 and C7) to long (on the left, C8 and C9). The second dimension explains 22.5% of variance and distinctly separates alcohols (blue, green) from ketones (red) and aldehydes (black). Functional group separation is clearer for short-chain than for long-chain molecules. The third dimension (right panel) explains 9.7% of variance and separates aldehydes (black) from other molecules. Altogether, odorants' chain length and functional group represent main coding dimensions for odorants in l-ALT projection neurons.

odorant than for presentations of different odorants (Fig. S1A, Paired t-test, $t = 11.0$, $p < 0.0001$, 13 df). Second, correlation coefficients were higher for odorants with the same functional group than for odorants with different functional groups (Fig. S1B, Paired t-test, $t = 5.88$, $p < 0.0001$). Lastly, correlation coefficients were also higher for odorants with the same carbon chain length compared to odorants with different carbon chain lengths (Fig. S1C, Paired t-test, $t = 4.46$, $p < 0.001$). As for Euclidian distances, this difference was significant when the odorants differed by at least 2 carbons (Fig. S1D, ANOVA $F_{3,39} = 47.05$, $p < 0.0001$; Tukey HSD test: a vs. b $p < 0.01$; a vs. c $p < 0.001$).

Comparison of honey bee and bumble bee data. The results we have described so far for bumble bees are generally very similar to the data obtained when imaging the homologous region of the honey bee AL[38,47]. We thus assessed the similarity of odor coding in bumble bees and honey bees by comparing odor-evoked intensity and similarity relationships between the two species. We performed linear regression analyses of response intensity (Fig. 7A) and similarity measures between bumble bees and honey bees (Fig. 7B).

Response intensities measured for the 16 odorants were highly correlated ($R^2 = 0.57$; $F_{1,14} = 18.64$, $p < 0.001$) showing that odorants inducing strong responses in bumble bees also induce strong activity in honey bees. This expected observation is a direct effect of response intensity directly depending on odorant vapor pressure in both species.

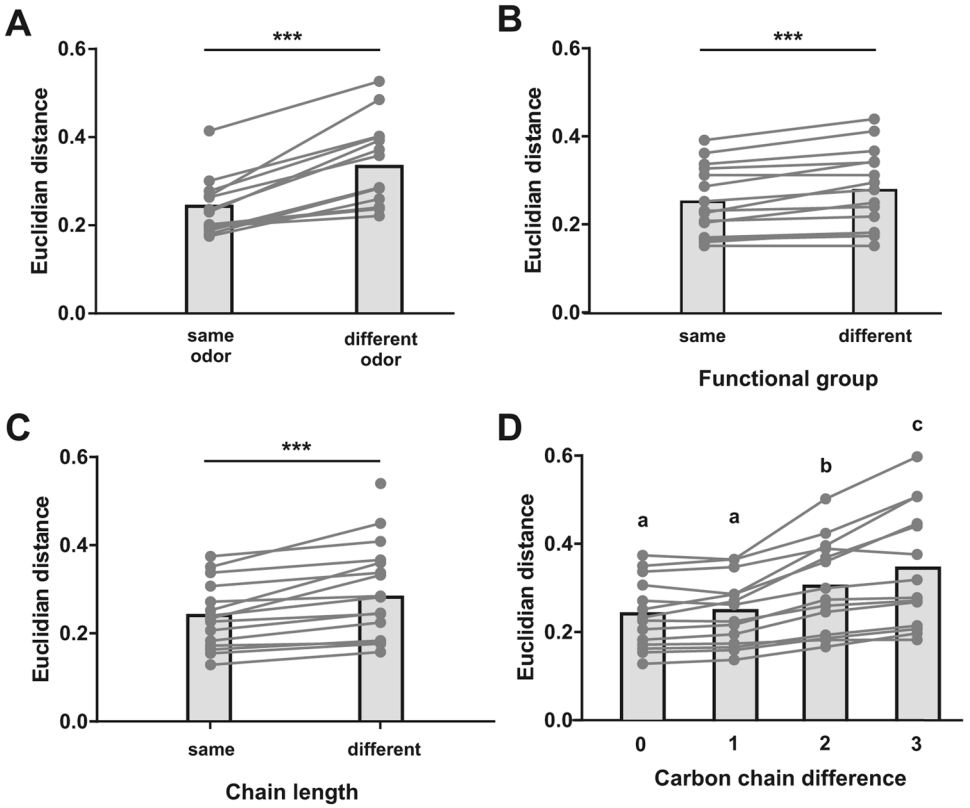

Figure 6. Odor quality coding depending on functional group or carbon chain length information. (**A**) Similarity (Euclidian distance) between presentations of the same or of different odorants. Activity maps are more similar when the same odorant is presented, showing specific odor coding in l-ALT projection neurons ($p < 0.001$). (**B**) Odorants with the same functional group induce more similar activity patterns than odorants with different functional groups ($p < 0.001$). (**C**) Odorants with the same chain length induce more similar activity patterns than odorants with different chain lengths ($p < 0.001$). (**D**) Similarity between odorants depending on the difference in their number of carbon atoms. Euclidian distances increase (i.e. response maps are more dissimilar) with increasing difference in the number of carbon atoms ($p < 0.001$; a vs. b, $p < 0.01$; a vs. c, $p < 0.001$; b vs. c, $p < 0.05$).

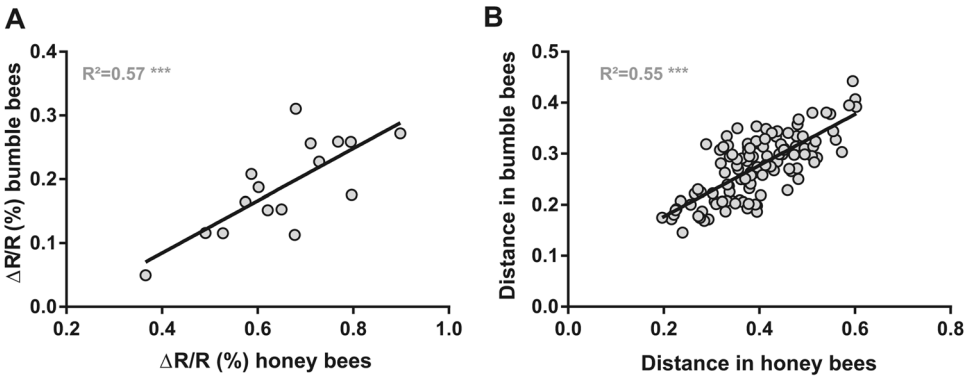

Figure 7. Comparison of odor coding in bumble bee and honey bee AL. (**A**) Correlation of response intensity for each of the 16 presented odorants between bumble bee (n = 14) and honey bee (n = 10) measures. A high and significant correlation is observed ($R^2 = 0.57$, $p < 0.001$). (**B**) Correlation of Euclidian distances between odor response maps for the 120 odorant pairs obtained in bumble bees and honey bees. A high and significant correlation is also observed ($R^2 = 0.55$, $p < 0.001$). Honey bee data from[38].

With regards to similarity relationships, Euclidian distances between odor response maps for the 120 odor pairs were strongly correlated between honey bees and bumble bees ($R^2 = 0.55$; Mantel test $p < 0.0001$). This result is illustrated by the similar arrangements of odorant representations observed in the multidimensional scaling analysis performed on bumble bee data (Fig. 5B) and in that previously performed on honey bee data (see Fig. 4A, l-ALT PNS, in[38]). Similarly, similarity measures based on correlation coefficients also yielded a significant correlation between honey bee and bumble bee data (data not shown; $R^2 = 0.21$; Mantel test $p < 0.005$). These results indicate that odorants inducing similar activity patterns in the honey bee AL also induce similar activity patterns in the bumble bee AL.

Discussion

This study shows that bumble bees are a suitable model organism for studying central olfactory processing and coding. Using neuroanatomical and neurophysiological approaches, we described AL architecture and measured glomerular activity patterns in response to odorants. We found that bumble bee l-ALT PNs provide clear information about odorants' chemical features, here their functional group and chain length. Although odor-evoked activity patterns were not topologically the same in bumble bees and honey bees, the general rules of olfactory coding in terms of intensity and similarity relationships were similar.

Neuroanatomical staining and 3D reconstructions indicated that the structure of the bumble bee AL greatly resembles that of the honey bee[45,49]. Both consist of a single layer of glomeruli around an inner coarse neuropil characterized by the presence of numerous local interneurons and projection neurons (see Fig. 1). The restricted innervation of the glomerular cortex by olfactory sensory neurons (OSN) seen in bumble bees is also reminiscent of the honey bee AL[45]. To note, in both species, a set of the most dorsal glomeruli innervated by the T4 tract present a homogeneous innervation compared with the exclusively peripheral innervation of the other glomeruli. The existence of the 4 OSN tracts in the bumble bee antennal lobe (Fig. 1B, plus 2 bypassing tracts towards dorsal lobe and subesophageal zone), and their similar arrangement to that observed in the honey bee[45,49] suggest a strong homology between the olfactory systems of both insects. The most prominent T1 tract innervates a large proportion of glomeruli on the rostro-ventral surface of the AL, which are directly accessible when opening the brain capsule. As in honey bees, these glomeruli could be stained retrogradely by placing dye crystals on the l-ALT tract of projection neurons (Fig. 2)[32,50]. We are thus confident that the group of glomeruli that we imaged in bumble bees is structurally homologous to the glomeruli usually imaged in honey bees with the same preparation[20,47,50].

Using in vivo optical recordings, we demonstrated that a panel of 16 aliphatic odorants evokes reproducible neuronal activity in the glomeruli of the bumble bee antennal lobe. In particular, we found that an odorant's functional group and chain length influence the intensity of odor-evoked signals, with primary alcohols inducing significantly lower activity than other functional groups, and short chain molecules activating glomeruli more strongly than molecules with longer chain lengths (Fig. 3). These effects, also found in honey bees[38,44,47] are explained by the strong correlation found between response intensity and odorant's vapor pressure. Thus, the bumble bee antennal lobe, as its honey bee counterpart, does not display any specific sensitivity for any of the odorants in our panel, and the intensity of AL activity mainly reflects odor concentration in vapor phase.

We then showed that each odorant evokes a specific glomerular activity pattern (Fig. 6A), which is different from that evoked by other odorants. Olfactory coding was influenced by both tested chemical features, carbon chain length and functional group, as previously observed both in invertebrates[38,44,47,51,52] and in mammals[53,54]. Odor-evoked activity within PNs is the product of OSN activity entering the AL and of local inhibitory networks carrying out local computations[38,50,55]. Despite a highly similar organization of their olfactory pathways, the main difference between honey bee and bumble bee systems lies in the repertoire of ORs expressed at the periphery. A recent study analyzed the genomes of two Bombus species, *Bombus terrestris* and *Bombus impatiens*[1] and aiming to identify key genes in the evolution of sociality, they compared the genomes of these species with that of the honey bee *Apis mellifera*. Concerning chemoreception, they found that *Bombus* genomes contain a slightly less numerous OR family than *Apis mellifera,* with 159 intact OR genes (excluding 5 pseudogenes). The number of glomeruli that we found in the AL of *Bombus terrestris* in our reconstructions ($n = 158 \pm 4$) corresponds well to the number of OR proteins found in the genome of this species, fitting with the general hypothesis in insects that each OSN expresses one type of odor-specific receptor, while all OSNs carrying the same receptor project to the same glomerulus in the AL[56]. This hypothesis is especially appealing as in honey bees the number of olfactory receptor genes largely coincides with the number of glomeruli in the AL (~ 165 glomeruli and ~ 163 intact OR genes excluding pseudogenes[57]). Note however, that in *Drosophila melanogaster,* several AL glomeruli are not innervated by OSNs expressing OR family genes, but rather by neurons expressing ionotropic receptors[58,59]. As bumble bee and honey bee genomes each contain about ~ 20 IR genes, with several orthologous genes, a proportion of their ALs may be innervated by IR expressing sensory neurons.

The comparison of the honey bee and the bumble bee OR family genes also showed duplications of genes in one or both species, several large species-specific gene lineage expansions, and at least 22 gene losses, reflecting the typical birth-and-death evolution of these receptors[7]. Recent evidence in different species of the genus *Drosophila* suggests that the number of olfactory receptor genes has remained quite similar for the entire period of *Drosophila* evolution (63 million years[60]), but that frequent gains and losses of genes occurred in each evolutionary lineage[61]. This may have changed the sequence of olfactory receptor neurons leading to different glomerular wiring patterns. The most recent common ancestors of honey bees and bumble bees are estimated to have lived between 70 and 90 million years ago[62–64]. This long time of separate evolution suggests that profound changes could also have taken place in the sequences of olfactory receptor genes in both species, modifying each receptor's sensitivity spectrum to odorant molecules, as well as the localization of its corresponding glomerulus in the AL. In accordance with these observations, direct comparison of odor-evoked activity patterns in bumble bees

and honey bees was difficult and we did not manage to identify possibly homologous glomeruli with a sufficient level of confidence (see Fig. S2 for an example).

Our finding of highly similar olfactory coding *rules,* supported by a clear coding of chain length and functional group information in bumble bees as in honey bees does not imply that ORs/glomeruli should be conserved between the two species. In our view, this finding is simply a by-product of the joined sensitivities and selectivities of the numerous OSN/ORs imaged simultaneously within each species. In a previous study, we showed that similarity relationships among inter-odorant maps measured in the ALs of an ant (*Camponotus fellah*) and the honey bee using calcium imaging were similar to those measured in the rat olfactory bulb using an utterly different recording technique (2-deoxyglucose autoradiography)[52]. The general rule was simple: odorants with a similar molecular structure (chain length and/or functional group) induced similar activity patterns in each insect's antennal lobe as well as in this mammal's olfactory bulb. More generally, it was observed that similarity relationships in a range of different species, including invertebrates and rodents, could be predicted to some extent based on purely molecular descriptors of odorants[65]. Thus, an emerging property of the multiple coding channels of each system (the ORs) which each detect a different but overlapping range of odorant molecule features is that neural representations mirror the chemical characteristics of the molecules. Importantly, this emerging property does not depend on the type of receptors expressed at the periphery since it is well established that olfactory receptor (OR) proteins in insects and vertebrates are unrelated[66,67]. Coming back to our study, honeybee and bumble bee ORs may well have evolved independently for a long time, our study shows that the two neural ensembles that were recorded in their ALs perform a reliable depiction of odorants' chemical features, granting these insects with a clear representation of odorants' structure. In honey bees, we previously showed that inter-odorant similarity relationships in the AL could predict bees' behavioral responses in a generalization protocol, so that similar odorants in the AL were treated as similar by the bees in their behavior[13,38,44]. The high correlation we found between odor-evoked response maps in the bumble bee and honeybee ALs suggests that bumble bees are indeed equipped, like honey bees, to respond to odorants according to chemical dimensions. We thus predict that future behavioral experiments in bumble bees shall reveal a similar organization of their olfactory perceptual space based on odorants chemical dimensions, as found in honey bees[13].

In conclusion, our study unravels a high similarity in the general organization of the primary olfactory processing center of bumble bees and honey bees. In addition, it shows similar olfactory coding rules conveying each system with a reliable depiction of odorants' chemical structure. While we concentrated here on the coding of general odorant features, we expect that future studies devoted to the coding of species-specific odorants, like social pheromones, may reveal more remarkable differences between both systems.

Methods

Bumble bee preparation. Medium-sized bumble bee *Bombus terrestris* workers were caught from an indoor colony (Koppert, Berkel en Rodenrijs, The Netherlands) and chilled on ice for 5 min until they stopped moving. Then, bumble bees were prepared following the standard preparation used to image the AL in honey bees[20,38,50]. In summary, the bumble bee's head was inserted and fixed in a plastic chamber with its antennae oriented to the front of the chamber. Using beeswax, the proboscis was flued at the front end of the holder to avoid movement of the brain during the experiment. Hairs on the top of the bumble bee head were removed and a pool was built with beeswax and pieces of plastic around the rostral part of the head capsule (behind the antennae). The pool was made waterproof with two-component epoxy glue (red Araldite, Bostik Findley, S.A.). A small window was then cut in the head cuticle from the bases of the antennae up to the ocelli, and glands as well as parts of the tracheal sheath were removed to expose the antennal lobes and parts of the protocerebrum. Finally, the pool was filled with some ringer solution (in mM: NaCl, 130; KCl, 6; $MgCl_2$, 4; $CaCl_2$, 5; sucrose, 160; glucose, 25; Hepes, 10; pH 6.7, 500 mOsmol; all chemicals from Sigma-Aldrich, Lyon, France), to avoid desiccation of the brain surface. Three hours prior to the experiment, a dye mixture was inserted into the brain with a broken borosilicate micropipette, aiming for the tract of l-ALT projection neurons, between the α lobe and the border of the optic lobe, rostrally from the lateral horn. The dye mixture consisted of the calcium-indicator Fura-2 dextran (10,000 kDa, Life technologies, France) and of tetramethylrhodamine dextran (10,000 kDa, Life technologies, France) for later anatomical observation, both in bovine serum albumin (2%).

Calcium imaging. In vivo optical recordings were performed as described elsewhere[22,38,68], with a T.I.L.L. Photonics imaging system (Martinsried, Germany), under an epifluorescence microscope (Olympus BX51WI) with a 10 × water-immersion objective (Olympus, UMPlanFL; NA 0.3), which was dipped into the ringer solution covering the brain. Only one AL was recorded in each bumble bee. Images were taken with a 640 × 480 pixels 12-bit monochrome CCD camera (T.I.L.L. Imago) cooled to -12 °C. Fura-2 was alternatively excited with 340 nm and 380 nm monochromatic light (T.I.L.L. Polychrom IV). Each measurement thus consisted of 50 double frames recorded at a rate of 5 Hz (integration time for each frame at 340 nm: 40–80 ms; for 380 nm: 10–20 ms) with 4 × 4 binning on chip (pixel image size corresponded to 4.8 µm × 4.8 µm). The filter set on the microscope contained a 490 nm dichroic filter and a bandpass (50 nm) 525 nm emission filter.

Odor presentation. A constant clean airstream, into which odor stimuli could be presented, was directed from a distance of 2 cm to the bumble bee's antennae. Odor stimuli (see below) were given at the 15th frame for 1 s (5 frames). Odor sources consisted in exchangeable Pasteur pipettes containing a piece of filter paper (1 cm^2) soaked with 5 µl of pure odorant (Sigma Aldrich, France).

In a first experiment, we tested 16 different aliphatic odorants that are part of floral blends bumble bees encounter while foraging[69]. The odorants differed systematically in terms of their carbon chain lengths (between 6 and 9 carbon atoms) and their functional groups (primary alcohol, secondary alcohol, aldehyde and ketone).

As control stimulus, we used a pipette containing a clean piece of filter paper without odor solution. This stimulus set was also used in a recent calcium imaging study of PN responses in the honey bee AL[38] allowing the comparison of odor coding in honey bees and bumble bees. The olfactory stimuli were presented three times in a pseudo-randomized order, avoiding consecutive stimuli to contain the same functional group or the same carbon chain length.

Data processing and analyses. A total of 50 bumble bees were imaged, out of which 14 presented high-quality signals and were kept for further analysis. Data were analyzed using custom-made software written in IDL 6.0 (Research Systems, Boulder, CO)[37]. Each odor presentation produced a four-dimensional array consisting of the excitation wavelength (340 or 380 nm), two spatial dimensions (x- and y-coordinates) along time (50 frames). First, the fluorescence ratio between excitation wavelengths at each pixel and time point was calculated: $R = F_{340nm}/F_{380nm}$. The relative fluorescence changes were then computed between the recorded odor responses R at each time point compared to the background fluorescence (before any odor presentation) R_0, defined as the average of the three images before odor stimulus onset (frames 12–14). Relative fluorescence changes were thus calculated as: $\Delta R = (R - R_0)/R_0$. The two spatial dimensions were then filtered with a gaussian filter of window size 7×7 pixels to reduce photon noise. Lastly, possible irregularities of lamp illumination were corrected by subtracting the median pixel value of each frame from each single pixel of the corresponding frame. The amplitude of the odor-induced response was calculated by subtracting the average of three consecutive frames during the odor presentation (frames 17–19) from the average of 3 frames before stimulus onset (frames 12–14). The response intensities presented as a function of the functional group or of the chain length of the odorants (Fig. 3B,C) were calculated by averaging within each animal the intensities recorded to the 4 odorants belonging to each group.

Activity maps (Fig. 2) represent the average amplitude observed over the three presentations of each odorant, in a false-color code, from dark blue (no signal) to red (maximum signal). As unambiguous identification of identical glomeruli across individual bumble bees was not feasible, odor coding was analyzed over the entire surface of the AL using a pixelwise analysis that avoids any bias due to glomerular misidentification. It was previously shown in honey bees that results based on the pixelwise method lead exactly to the same conclusions as glomerular identification[37]. For each bee, a mask was precisely drawn along the edges of the AL to limit the measure of odor-evoked responses to the glomerular area. Global glomerular activity upon odor stimulation was measured by averaging the intensity values of all pixels within the unmasked area. Evaluation of (dis-)similarity relationships between odorant representations was performed by calculating pixelwise Euclidian distances for all pairs of the 16 odorant stimuli used (120 odor pairs). For all analyses, average values for the three presentations of each odorant were used except for the comparison of Euclidian distances for the *same or different* odorants (Fig. 6A and Fig. S1A), where each single odorant presentation was used.

Anatomical staining. For antennal staining of the whole antennal lobe, the scapes of the antennae were carefully opened using a microscalpel, and the antennal nerve was cut with a borosilicate micropipette coated with tetramethylrhodamine dextran (10,000 kDa, Life technologies, France). Afterwards, animals were kept in a cool place until the next day to allow the dye to migrate to the AL and to stain OSN processes within the glomeruli. The brains were removed and fixed in 4% paraformaldehyde solution for at least 24 h. They were then dehydrated in ascending concentrations of ethanol, cleared and stored in methyl salicylate (Sigma-Aldrich, Lyon, France). Images of the tetramethylrhodamine-stained glomeruli were taken using a confocal laser scanning microscope (Zeiss, LSM 700) with a W Plan-Apochromat 20x/1.0 objective and a 555 nm excitation wavelength at 2 µm optical section thickness and pixel size of 0.31 µm × 0.31 µm. Recorded stacks of images were adjusted in brightness and contrast using imageJ (Rasband; National Institutes of Health, Bethesda, MD). Segmentation and anatomical reconstruction of the antennal lobe was performed using Amira (version 4.5.1 Mercury Computer Systems, Merignac, France). The neuraxis was used for all anatomical descriptions[70,71].

After successful calcium imaging, the brains were removed and the same techniques as described above were used.

Statistical analysis. Normality of the data was tested and confirmed for almost all data points using Shapiro–Wilk normality test. We thus applied parametric statistics over the whole study. When normality was not achieved for all data points in an analysis, the corresponding non-parametric test was performed. In all cases, both types of tests gave the same result, and therefore the text only describes parametric results. The intensities of responses to the different odorants were compared using ANOVA for repeated measurements. When significant, Dunnett's test was applied to compare the intensity of each response to a common reference, the air control. Odor-evoked response intensities between functional groups and chain lengths were compared using ANOVA for repeated measurements, followed by Tukey post-hoc tests for further analysis of statistically significant main effects. Paired t-tests were applied to compare Euclidian distances obtained for different presentations of the same odor versus presentations of different odors, as well as for odors with the same or with a different functional group or chain length. A Pearson correlation analysis was performed between response intensity and the logarithm of odorants' vapor pressure. In some analyses (Fig. 7), data recorded in bumble bees were compared to data recorded in honey bees[38], using exactly the same experimental and analytical procedures. A Pearson correlation analysis thus evaluated a possible correlation of odor-response intensities between the two species. A Mantel test was used to evaluate a possible correlation between bumble bee and honey bee Euclidian distance matrices. All tests were performed with GraphPad Prism (version 7, GraphPad software) or R (www.r-project.org). All values are displayed as means ± SEM.

Data availability

All data are available upon request from the corresponding author.

Received: 1 December 2020; Accepted: 10 May 2021
Published online: 26 May 2021

References

1. Sadd, B. M. *et al.* The genomes of two key bumblebee species with primitive eusocial organization. *Genome Biol.* **16**, 76 (2015).
2. Jandt, J. M., Huang, E. & Dornhaus, A. Weak specialization of workers inside a bumble bee (Bombus impatiens) nest. *Behav. Ecol. Sociobiol.* **63**, 1829–1836 (2009).
3. von Frisch, K. *The Dance Language and Orientation of Bees* (Harvard University Press, 1967).
4. Molet, M., Chittka, L. & Raine, N. E. How floral odours are learned inside the bumblebee (Bombus terrestris) nest. *Naturwissenschaften* **96**, 213–219 (2009).
5. Dornhaus, A. *et al.* (Google Patents, 2009).
6. Dornhaus, A. & Chittka, L. Food alert in bumblebees (Bombus terrestris): possible mechanisms and evolutionary implications. *Behav. Ecol. Sociobiol.* **50**, 570–576 (2001).
7. Ramdya, P. & Benton, R. Evolving olfactory systems on the fly. *Trends Genet.* **26**, 307–316. https://doi.org/10.1016/j.tig.2010.04.004 (2010).
8. Sandoz, J. C. Behavioral and neurophysiological study of olfactory perception and learning in honeybees. *Front Syst Neurosci* **5**, 98. https://doi.org/10.3389/fnsys.2011.00098 (2011).
9. Galizia, C. G., Eisenhardt, D. & Giurfa, M. *Honeybee Neurobiology and Behavior: A Tribute to Randolf Menzel* (Springer Science & Business Media, 2011).
10. Giurfa, M. Behavioral and neural analysis of associative learning in the honeybee: a taste from the magic well. *J. Comp. Physiol. A.* **193**, 801–824 (2007).
11. Menzel, R. The honeybee as a model for understanding the basis of cognition. *Nat. Rev. Neurosci.* **13**, 758–768. https://doi.org/10.1038/nrn3357 (2012).
12. Nouvian, M., Hotier, L., Claudianos, C., Giurfa, M. & Reinhard, J. Appetitive floral odours prevent aggression in honeybees. *Nat. Commun.* **6**, 10247. https://doi.org/10.1038/ncomms10247 (2015).
13. Guerrieri, F., Schubert, M., Sandoz, J. C. & Giurfa, M. Perceptual and neural olfactory similarity in honeybees. *PLoS Biol.* **3**, e60 (2005).
14. Vareschi, E. Duftunterscheidung bei der Honigbiene: Einzelzell-Ableitungen und Verhaltensreaktionen. *Zeitschrift fur vergleichende Physiologie* **75**, 143–173 (1971).
15. Kirschner, S. *et al.* Dual olfactory pathway in the honeybee, Apis mellifera. *J. Comp. Neurol.* **499**, 933–952 (2006).
16. Nishino, H., Nishikawa, M., Mizunami, M. & Yokohari, F. Functional and topographic segregation of glomeruli revealed by local staining of antennal sensory neurons in the honeybeeApis mellifera. *J. Comp. Neurol.* **515**, 161–180. https://doi.org/10.1002/cne.22064 (2009).
17. Mobbs, P. G. The brain of the honeybee Apis mellifera I: the connections and spatial organization of the mushroom bodies. *Philos. Trans. R. Soc. Lond. B* **298**, 309–354 (1982).
18. Brill, M. F. *et al.* Parallel processing via a dual olfactory pathway in the honeybee. *J. Neurosci.* **33**, 2443–2456. https://doi.org/10.1523/JNEUROSCI.4268-12.2013 (2013).
19. Kropf, J. & Rössler, W. In-situ recording of ionic currents in projection neurons and Kenyon cells in the olfactory pathway of the honeybee. *PLoS ONE* **13**, e0191425. https://doi.org/10.1371/journal.pone.0191425 (2018).
20. Joerges, J., Küttner, A., Galizia, C. G. & Menzel, R. Representations of odours and odour mixtures visualized in the honeybee brain. *Nature* **387**, 285–288 (1997).
21. Szyszka, P., Galkin, A. & Menzel, R. Associative and non-associative plasticity in Kenyon cells of the honeybee mushroom body. *Front. Syst. Neurosci.* **2**, 3 (2008).
22. Mota, T., Gronenberg, W., Giurfa, M. & Sandoz, J. C. Chromatic processing in the anterior optic tubercle of the honey bee brain. *J. Neurosci.* **33**, 4–16. https://doi.org/10.1523/JNEUROSCI.1412-12.2013 (2013).
23. Paoli, M. *et al.* Neuronal response latencies encode first odor identity information across subjects. *J. Neurosci.* **38**, 9240–9251 (2018).
24. Jernigan, C. M. *et al.* Experience-dependent tuning of early olfactory processing in the adult honey bee, *Apis mellifera*. *J. Exp. Biol.* **223**, 1–13. https://doi.org/10.1242/jeb.206748 (2020).
25. Riveros, A. J. & Gronenberg, W. Olfactory learning and memory in the bumblebee Bombus occidentalis. *Naturwissenschaften* **96**, 851–856 (2009).
26. Sommerlandt, F. M., Rössler, W. & Spaethe, J. Elemental and non-elemental olfactory learning using PER conditioning in the bumblebee, Bombus terrestris. *Apidologie* **45**, 106–115 (2014).
27. Leonard, A. S. & Masek, P. Multisensory integration of colors and scents: insights from bees and flowers. *J. Comp. Physiol. A.* **200**, 463–474 (2014).
28. Laloi, D. *et al.* Olfactory conditioning of the proboscis extension in bumble bees. *Entomogia Experimentalis et Applicata* **90**, 123–129 (1999).
29. Smith, D. B. *et al.* Exploring miniature insect brains using micro-CT scanning techniques. *Sci. Rep.* **6**, 21768 (2016).
30. Paulk, A. C., Phillips-Portillo, J., Dacks, A. M., Fellous, J.-M. & Gronenberg, W. The processing of color, motion, and stimulus timing are anatomically segregated in the bumblebee brain. *J. Neurosci.* **28**, 6319–6332 (2008).
31. Mares, S., Ash, L. & Gronenberg, W. Brain allometry in bumblebee and honey bee workers. *Brain Behav. Evol.* **66**, 50–61 (2005).
32. Strube-Bloss, M. F., Brown, A., Spaethe, J., Schmitt, T. & Rössler, W. Extracting the behaviorally relevant stimulus: unique neural representation of farnesol, a component of the recruitment pheromone of Bombus terrestris. *PLoS ONE* **10**, e0137413 (2015).
33. Fonta, C. & Masson, C. Organisation neuroanatomique de la voie afferente antennaire chez les bourdons males et femelles (Bombus sp.). *Comptes rendus des séances de l'Académie des sciences Série 3, Sciences de la vie* **300**, 437–442 (1985).
34. Hansson, B. S. & Anton, S. Function and morphology of the antennal lobe: new developments. *Ann. Rev. Entomol.* **45**, 203–231 (2000).
35. Meyer, A., Galizia, C. G. & Nawrot, M. P. Local interneurons and projection neurons in the antennal lobe from a spiking point of view. *J. Neurophysiol.* **110**, 2465–2474 (2013).
36. Abel, R., Rybak, J. & Menzel, R. Structure and Response Patterns of Olfactory Interneurons in the Honeybee, Apis mellifera. *J. Comp. Neurol.* **437**, 363–383 (2001).
37. Carcaud, J., Giurfa, M. & Sandoz, J. C. Differential combinatorial coding of pheromones in two olfactory subsystems of the honey bee brain. *J. Neurosci.* **35**, 4157–4167. https://doi.org/10.1523/JNEUROSCI.0734-14.2015 (2015).
38. Carcaud, J., Giurfa, M. & Sandoz, J. C. Differential Processing by two olfactory subsystems in the honeybee brain. *Neuroscience* **374**, 33–48. https://doi.org/10.1016/j.neuroscience.2018.01.029 (2018).

39. Fonta, C. & Masson, C. Comparative study by electrophysiology of olfactory responses in bumblebees (Bombus hypnorum and-Bombus terrestris). *J. Chem. Ecol.* **10**, 1157–1168 (1984).
40. Fonta, C. & Masson, C. Structural and functional studies of the peripheral olfactory nervous system of male and female bumblebees (Bombus hypnorum and Bombus terrestris). *Chem. Senses* **12**, 53–69. https://doi.org/10.1093/chemse/12.1.53 (1987).
41. Spaethe, J., Brockmann, A., Halbig, C. & Tautz, J. Size determines antennal sensitivity and behavioral threshold to odors in bumblebee workers. *Naturwissenschaften* **94**, 733–739. https://doi.org/10.1007/s00114-007-0251-1 (2007).
42. Anfora, G. *et al.* Lateralization in the invertebrate brain: left-right asymmetry of olfaction in bumble bee, Bombus terrestris. *PLoS ONE* **6**, e18903. https://doi.org/10.1371/journal.pone.0018903 (2011).
43. Okada, K. & Kanzaki, R. Localization of odor-induced oscillations in the bumblebee antennal lobe. *Neurosci. Lett.* **316**, 133–136 (2001).
44. Carcaud, J., Hill, T., Giurfa, M. & Sandoz, J. C. Differential coding by two olfactory subsystems in the honeybee brain. *J. Neurophysiol.* **108**, 1106–1121 (2012).
45. Galizia, C. G., McIlwrath, S. L. & Menzel, R. A digital three-dimensional atlas of the honeybee antennal lobe based on optical sections aquired using confocal microscopy. *Cell Tissue Res.* **295**, 383–394 (1999).
46. Kelber, C., Rössler, W. & Kleineidam, C. J. Multiple olfactory receptor neurons and their axonal projections in the antennal lobe of the honeybee Apis mellifera. *J. Comp Neurol.* **496**, 395–405 (2006).
47. Sachse, S., Rappert, A. & Galizia, C. G. The Spatial representation of chemical structures in the antennal lobe of honeybees: steps towards the olfactory code. *Eur. J. Neurosci.* **11**, 3970–3982 (1999).
48. Mardia, K. V. Some properties of clasical multi-dimesional scaling. *Commun. Stat. Theory Methods* **7**, 1233–1241 (1978).
49. Flanagan, D. & Mercer, A. R. An atlas and 3-D reconstruction of the antennal lobes in the worker honey bee, Apis mellifera L. (Hymenoptera: Apidae). *Int. J. Insect. Morphol. Embryol.* **18**, 145–159 (1989).
50. Sachse, S. & Galizia, C. G. The role of inhibition for temporal and spatial odor representation in olfactory output neurons: a calcium imaging study. *J. Neurophysiol.* **87**, 1106–1117 (2002).
51. Couto, A., Alenius, M. & Dickson, B. J. Molecular, anatomical, and functional organization of the Drosophila olfactory system. *Curr. Biol.* **15**, 1535–1547 (2005).
52. Dupuy, F., Josens, R., Giurfa, M. & Sandoz, J. C. Calcium imaging in the ant Camponotus fellah reveals a conserved odour-similarity space in insects and mammals. *BMC. Neurosci.* **11**, 28 (2010).
53. Johnson, B. A. & Leon, M. Chemotopic odorant coding in a mammalian olfactory system. *J. Comp. Neurol.* **503**, 1–34 (2007).
54. Mori, K., Takahashi, Y. K., Igarashi, K. M. & Yamaguchi, M. Maps of odorant molecular features in the Mammalian olfactory bulb. *Physiol. Rev.* **86**, 409–433 (2006).
55. Sachse, S. & Galizia, C. G. The coding of odour-intensity in the honeybee antennal lobe: local computation optimizes odour representation. *Eur. J. Neurosci.* **18**, 2119–2132 (2003).
56. Vosshall, L. B., Wong, A. M. & Axel, R. An olfactory sensory map in the fly brain. *Cell* **102**, 147–159 (2000).
57. Robertson, H. M. & Wanner, K. W. The chemoreceptor superfamily in the honey bee, Apis mellifera: expansion of the odorant, but not gustatory, receptor family. *Genome Res.* **16**, 1395–1403 (2006).
58. Silbering, A. F. *et al.* Complementary function and integrated wiring of the evolutionarily distinct Drosophila olfactory subsystems. *J. Neurosci.* **31**, 13357–13375 (2011).
59. Grabe, V. *et al.* Elucidating the neuronal architecture of olfactory glomeruli in the drosophila antennal lobe. *Cell Rep.* **16**, 3401–3413. https://doi.org/10.1016/j.celrep.2016.08.063 (2016).
60. Tamura, K., Subramanian, S. & Kumar, S. Temporal patterns of fruit fly (Drosophila) evolution revealed by mutation clocks. *Mol. Biol. Evol.* **21**, 36–44. https://doi.org/10.1093/molbev/msg236 (2004).
61. Nozawa, M. & Nei, M. Evolutionary dynamics of olfactory receptor genes in Drosophila species. *Proc. Natl. Acad. Sci. U S A* **104**, 7122–7127. https://doi.org/10.1073/pnas.0702133104 (2007).
62. Michener, C. D. & Grimaldi, D. A. The oldest fossil bee: Apoid history, evolutionary stasis, and antiquity of social behavior. *Proc. Natl. Acad. Sci. U S A* **85**, 6424–6426. https://doi.org/10.1073/pnas.85.17.6424 (1988).
63. Schultz, T. R., Engel, M. S. & Aschier, J. S. Evidence for the origin of eusociality in the corbiculate bees (Hymenoptera: Apidae). *Journal of the Kansas Entomological Society*, 10–16 (2001).
64. Ramírez, S. R., Roubik, D. W., Skov, C. & Pierce, N. E. Phylogeny, diversification patterns and historical biogeography of euglossine orchid bees (Hymenoptera: Apidae). *Biol. J. Lin. Soc.* **100**, 552–572. https://doi.org/10.1111/j.1095-8312.2010.01440.x (2010).
65. Haddad, R. *et al.* A metric for odorant comparison. *Nat. Methods* **5**, 425–429 (2008).
66. Benton, R. Multigene family evolution: perspectives from insect chemoreceptors. *Trends Ecol. Evol.* **30**, 590–600. https://doi.org/10.1016/j.tree.2015.07.009 (2015).
67. Benton, R., Sachse, S., Michnick, S. W. & Vosshall, L. B. Atypical membrane topology and heteromeric function of Drosophila odorant receptors in vivo. *PLoS. Biol.* **4**, e20 (2006).
68. Roussel, E., Carcaud, J., Combe, M., Giurfa, M. & Sandoz, J. C. Olfactory coding in the honeybee lateral horn. *Curr. Biol.* **24**, 561–567. https://doi.org/10.1016/j.cub.2014.01.063 (2014).
69. Knudsen, J. T., Tollsten, L. & Bergström, L. G. Floral scents: a checklist of volatile compounds isolated by head-space techniques. *Phytochemistry* **33**, 253–280 (1993).
70. Strausfeld, N. J. Organization of the honey bee mushroom body: representation of the calyx within the vertical and gamma lobes. *J. Comp. Neurol.* **450**, 4–33 (2002).
71. Kreissl, S., Strasser, C. & Galizia, C. G. Allatostatin immunoreactivity in the honeybee brain. *J. Comp. Neurol.* **518**, 1391–1417 (2010).

Acknowledgements

The study was supported by the Deutsche Forschungsgemeinschaft (DFG). We thank Pr. Martin Egelhaaf for providing additional financial support for M.M. We are grateful to Maud Combe for developing the custom programs used for data analysis. We thank the ANR (Projects 2010-BLAN-1712-01 and ANR-17-CE20-003 to J.C.S.) and the French Research Ministry (J.C.). We also would like to thank Antoine Couto and Manon Lefèvre Houard for their help with the anatomical reconstruction.

Author contributions

A preliminary version of this work appeared in the doctoral thesis of the first author (Universität Bielefeld, 2013). M.M., J.C., M.E. and J.C.S. conceived the experiments. M.M. collected the data. M.M., J.C. and J.C.S. analyzed the data and interpreted the results. M.M, J.C. and J.C.S. wrote the manuscript. All authors read and approved the final version of the manuscript.

Competing interests

The authors declare no competing interests.

Additional information

Supplementary Information The online version contains supplementary material available at https://doi.org/10.1038/s41598-021-90400-6.

Correspondence and requests for materials should be addressed to J.C.

Reprints and permissions information is available at www.nature.com/reprints.

Publisher's note Springer Nature remains neutral with regard to jurisdictional claims in published maps and institutional affiliations.